

# ENERGETIC ASPECTS IN CLASSICAL PULSATORS

Marc-Antoine Dupret<sup>\*1</sup>, A. Grigahcène<sup>2</sup>, S. Théado<sup>3</sup>, P.-O. Bourge<sup>3</sup>, and M. Gabriel<sup>3</sup>

<sup>1</sup>*Observatoire de Paris, LESIA, CNRS UMR 8109, 92195 Meudon, France*

<sup>2</sup>*CRAAG - Algiers Observatory BP 63 Bouzareah 16340, Algiers, Algeria*

<sup>3</sup>*Institut d'Astrophysique et de Géophysique, Université de Liège, Belgium*

## ABSTRACT

We consider the energetic aspects of pulsations in auto-driven main sequence stars. The problems of the modeling of the coherent interaction between convection and oscillations and the transfer in the pulsating atmosphere are discussed. We analyze the driving mechanisms at the origin of the pulsations in different types of main sequence variable stars: the  $\beta$  Cephei, the Slowly Pulsating B (SPB), the  $\delta$  Scuti, the roAp and the  $\gamma$  Doradus stars. We also consider the problem of the determination of the theoretical amplitude ratios and phase differences, which is very important for the mode identification.

Key words: Asteroseismology; Convection;  $\beta$  Cep; SPB;  $\delta$  Sct; roAp;  $\gamma$  Dor.

## 1. INTRODUCTION

It is known that adiabaticity can be reasonably assumed for the determination of the oscillation frequencies. However, the oscillations are always completely non-adiabatic in the superficial layers of a star, where the thermal relaxation time is smaller than the pulsation periods. In these regions, the dynamical and thermal equations for the oscillations are coupled and must be solved together. The solution of these equations can be obtained with a non-adiabatic pulsation code, allowing the study of energetic aspects of the oscillations. In particular, the driving of the modes for classical pulsators can be studied (solar-like oscillations are not considered here, we refer to Houdek et al. and Samadi et al., these proceedings). There is the well known  $\kappa$ -mechanism and others associated for example with the flux blocking at the base of the convective envelope. We present a review of these mechanisms in different types of main sequence variable stars, with special stress on the information they give us on the physics of stellar interiors. Another important field is the interpretation of the amplitudes and phases at the photosphere. The amplitude ratios and phase differences of magnitude variations in different photometric passbands or between

the light and velocity curves can be determined with non-adiabatic linear computations. The comparison with observations allows the identification of the degree  $\ell$  and gives constraints on the description of the superficial layers and thermal aspects of the oscillations. These additional constraints are complementary with those obtained by classical frequency fitting.

## 2. NON-ADIABATIC MODELS

In the full non-adiabatic case and in the linear approximation, the oscillation modes are the solutions of a complex eigenvalue problem of the 6th order (neglecting here non-locality). The equations to be solved are the perturbed equations of mass, momentum and energy conservation, the perturbed Poisson and transfer equations. Two difficult problems in this framework are the modeling of the perturbed convective quantities (convective flux, Reynolds stress, ...) and the transfers in the pulsating atmosphere. We summarize here these two problems and propose some solutions.

### 2.1. Convection-oscillations interaction

There are different approaches for the study of the convection-pulsation interaction. First, 3D hydrodynamical simulations can be performed. All motions, and thus in particular the acoustic modes are present in the turbulence spectrum. Hence, the analysis of such simulations could enable us in principle to study the energetics of the oscillations inside a convective zone. However, these simulations (e.g. Stein & Nordlund 1998) are highly computer time consuming and are restricted to the thin upper part of the convection zone. At present they enable us to study only the incoherent contribution of the convection to the oscillations energetics. As an example, they can be used to determine the power injected in the acoustic modes for stochastically excited oscillators (Samadi et al. 2003).

But the damping rates of the modes in solar-like oscillators or their growth rates in auto-driven oscillators ( $\delta$  Sct,  $\gamma$  Dor stars, ...) as well as the amplitude and phases

\*Chargé de Recherche de 1ère classe, CNRS

cannot be determined by this approach. The only present way to determine these quantities is throughout an analytical perturbative approach.

As the study of the coherent interaction between convection and oscillations is a difficult problem, an approximation which is often adopted is the frozen convection. It must be stressed that there are different ways to freeze the convection: neglecting the Lagrangian or Eulerian variations of the convective flux, the convective luminosity, or the divergence of the convective flux . . . The frozen convection approximation is a reasonable approximation when the time scale of most energetic convective motions is larger than the pulsation periods, but this is never the case in the whole convective envelope.

As this approximation is not justified in many cases, Time-Dependent Convection (TDC) treatments have been derived for the modeling of the coherent interaction between convection and oscillations. In these approaches, the acoustic and convective motions are separated by assuming that the first have much larger wavelengths than the last ones in the spectrum of turbulence. Examples of TDC theories are those of Gough (1977) and Gabriel (1996) which are based on the Mixing-Length (ML) approach, and the theory of Xiong (1997) which is more sophisticated.

The theory of Gabriel (1996) is the only one valid for non-radial modes and we consider it with more details in this paper. As usually in the study of turbulence, the different physical quantities are separated into a mean part and a convective fluctuation part. We obtain then hydrodynamic equations for the average medium and for the convective fluctuations. The perturbation of the mean equations gives the linear equations for the non-adiabatic oscillations. But in these equations appear unknown perturbed correlation terms: the perturbations of the convective flux, the Reynolds stress tensor and the dissipation rate of turbulent kinetic energy into heat. These terms are obtained by perturbing the equations for the convective fluctuations. In order to have as much equations as variables, it is necessary to add some closure equations. In the mixing-length approach, the problem is closed immediately by introducing an ad-hoc life-time of the convective elements  $\tau_c$ . We refer to Grigahcène et al. (2005) (G05) and paper II of Dupret et al. (these proceedings) for more details on the underlying equations.

In the stationary case, this approach leads to the classical MLT equations adopted in most of the stellar evolution codes. The things are however more complex when we consider the perturbation of turbulence due to the oscillations. The problem is that all the turbulence cascade is hidden behind the closure terms and their perturbation is subject to large uncertainties, these questions are detailed in G05 and paper II. Another important problem is the modeling of the non-local nature of turbulence. It must be stressed that in some cases such as solar-like oscillations, the non-locality affects strongly the results (see the other papers of Dupret et al., these proceedings, and Balmforth 1992). Finally, differential equations can be

obtained relating the perturbed convective quantities such as the convective flux and the turbulent pressure to the usual eigenfunctions (perturbations of entropy and pressure, displacement, . . .). These equations are substituted in the general system for the linear non-adiabatic stellar oscillations, and the full problem can be solved with a non-adiabatic pulsation code.

## 2.2. Transfer in the pulsating atmosphere

The non-adiabatic modeling of the transfers in the pulsating atmosphere is also a difficult problem. The perturbed radiative flux can no longer be obtained using the diffusion approximation. In all generality we would have to perturb and solve the full transfer equations for all wavelengths. Some approaches have been proposed, but they are still too complex to be implemented in non-adiabatic pulsation codes.

To avoid these difficulties, simpler approaches have been proposed. The simplest is to solve the problem in the interior only, using the diffusion approximation, and to impose as thermal boundary condition at the photosphere ( $\tau = 2/3$ ):  $\delta F/F = 4\delta T/T$ . But this is a very crude approximation as it neglects the significant variation of the optical depth at the photosphere. Another approach is to adopt a perturbed form of the Eddington approximation in the atmosphere (see e.g. Saio & Cox 1980). Finally, another simple approach was proposed by Dupret et al. (2002). The main idea is that the thermal relaxation time of the atmosphere (some seconds) is much smaller than the typical pulsation periods. Hence it can be assumed in good approximation that the atmosphere will keep the same thermal structure as equilibrium atmosphere models. We obtain then the following equations:

$$\frac{\delta T}{T} = \frac{\partial \ln T}{\partial \ln T_{\text{eff}}} \frac{\delta T_{\text{eff}}}{T_{\text{eff}}} + \frac{\partial \ln T}{\partial \ln g_e} \frac{\delta g_e}{g_e} + \frac{\partial \ln T}{\partial \ln \tau} \frac{\delta \tau}{\tau}, \quad (1)$$

$$\frac{\partial \delta \tau}{\partial \tau} = \frac{\delta \kappa}{\kappa} + \frac{\delta \rho}{\rho} + \frac{\partial \xi_r}{\partial r}. \quad (2)$$

Eliminating  $\delta \tau$  between these two equations gives a new differential equation to be used instead of the perturbed diffusion equation. A big advantage of this treatment is that it can be used with any type of atmosphere model (e.g. Kurucz 1993). We refer for example to the paper of Baudin et al. (these proceedings), where non-adiabatic computations were performed using the VAL solar atmosphere model including the very superficial chromospheric layers with increasing temperatures towards the surface.

The perturbed treatment adopted in the atmosphere affects mainly the determination of the theoretical amplitude ratios and phase differences at the photosphere. The driving of the modes is less sensitive to this treatment, at least for stars in which sufficiently deep layers (Fe, HeII partial ionization zones) play the major driving role.

### 3. DRIVING MECHANISMS

Non-adiabatic computations allow the study of the driving mechanisms of the modes. In the linear formalism, the time dependence of a pulsation mode is of the form  $e^{\eta+ist}$ , where  $\eta$  is the growth or damping rate of the modes (positive for overstable modes, negative for stable ones). In this section, we discuss the physical mechanisms determining  $\eta$  and thus the vibrational stability of pulsation modes.

#### 3.1. $\kappa$ -mechanism

$\eta$  is the solution of an integral expression. For the sake of clarity of the discussion, we begin with a simplified expression obtained in the quasi-adiabatic case, for a radial mode, neglecting time-dependent convection and the perturbation of nuclear reactions:

$$\eta = -\frac{\mathcal{P}}{2\sigma_0^2\mathcal{I}} = -\frac{1}{2\sigma_0^2} \frac{\int_0^M \frac{\delta T}{T} \frac{d\delta L}{dm} dm}{\int_0^M \xi_r^2 dm}, \quad (3)$$

where  $\mathcal{P}$  is the mean power performed by the system,  $\mathcal{I}$  is the inertia of the mode and  $\sigma_0^2\mathcal{I}$  the energy of the mode. From Eq. (3), we see that the regions where  $\delta L$  is decreasing outwards at the hot phase ( $\delta T > 0$ ) have a driving effect on the stellar pulsations. When this occurs, the pulsating star can be compared with a heat engine, we have a motor thermodynamic cycle in which energy is taken by the system at the hot phase and released at the cold phase. On the contrary, the regions where  $\delta L$  is increasing outwards at the hot phase have a damping effect. For a radial mode and a frozen convective luminosity, the perturbed luminosity is given by:

$$\frac{\delta L}{L} = \frac{L_R}{L} \left( 4 \frac{\xi_r}{r} + 3 \frac{\delta T}{T} - \frac{\delta \kappa}{\kappa} + \frac{\partial \delta T / \partial r}{dT/dr} \right). \quad (4)$$

This enables us to understand the well known  $\kappa$ -mechanism. We focus on the opacity term  $-\delta\kappa/\kappa$  which plays in general a dominant role on the variation of the luminosity. In the quasi adiabatic approximation, we can write:

$$\frac{\delta \kappa}{\kappa} = \kappa_{PS} \frac{\delta P}{P} = \frac{(\Gamma_3 - 1)\kappa_T + \kappa_\rho}{\Gamma_1} \frac{\delta P}{P}. \quad (5)$$

In usual circumstances (e.g. Kramers opacity law, complete ionization) we have  $\kappa_{PS} \simeq -0.8$ . Since  $\delta P/P$  is generally increasing outwards at the hot phase, the contribution of  $-\delta\kappa/\kappa$  in Eq. (4) implies that  $\delta L/L$  is increasing outwards at the hot phase, which has a damping effect on the pulsation.

However, in the superficial layers of a star, large opacity bumps are present in the regions of partial ionization. In parts of these regions,  $\kappa_{PS}$  is increasing very steeply outwards and can take positive values. Therefore, in these regions, the contribution of  $-\delta\kappa/\kappa$  implies that  $\delta L/L$  is decreasing outwards at the hot phase, the energy is blocked because of this opacity variation, and this has a driving effect on the pulsations. This mechanism is called the  $\kappa$ -mechanism. We note that the adiabatic exponent  $\Gamma_3$  drops in these partial ionization zones, and this can also affect the driving mechanism, called in this case  $\kappa$ - $\gamma$ -mechanism. The  $\kappa$ -mechanism is efficient when a partial ionization zone is located exactly in the transition region where the thermal relaxation time is of the same order as the pulsation period. The conjunction between these two zones determines the exact location of the instability regions throughout the HR diagram.

#### 3.2. Role of time-dependent convection (TDC)

When TDC is taken into account, the integral expression for the mean power is more complex. For radial modes, it has the following form:

$$\begin{aligned} \mathcal{P} = & - \int_0^m (\Gamma_3 - 1) \Re \left\{ \frac{\delta \rho^*}{\rho} \frac{d(\delta L_R + \delta L_c)}{dm} \right\} dm \\ & - \int_0^m \sigma \Im \left\{ \frac{\delta \rho^*}{\rho} \frac{\delta p_t}{\rho} \right\} dm \\ & + \int_0^m (\Gamma_3 - 1) \Re \left\{ \frac{\delta \rho^*}{\rho} \delta \left( \epsilon_2 + \vec{V} \cdot \frac{\nabla p}{\rho} \right) \right\} dm \quad (6) \end{aligned}$$

In this expression, different new terms appear. In addition to the radiative luminosity variations ( $\delta L_R$ ) discussed in previous section, we see the role played by the convective luminosity variations ( $\delta L_c$ ) the turbulent pressure variations ( $\delta p_t$ ) and the dissipation rate of turbulent kinetic energy variations. This last term takes the following expression for isotropic turbulence:

$$\Re \left\{ \frac{\delta \rho^*}{\rho} \delta \left( \epsilon_2 + \vec{V} \cdot \frac{\nabla p}{\rho} \right) \right\} = \frac{3}{2} \sigma \Im \left\{ \frac{\delta \rho^*}{\rho} \frac{\delta p_t}{\rho} \right\}. \quad (7)$$

We see from this equation that the perturbation of turbulent pressure (in the movement equation) and the perturbation of dissipation rate of turbulent kinetic energy (in the energy equation) have opposite effects on the work integral and thus on the excitation and damping of the modes. In particular, if the gas is completely ionized and radiative pressure is negligible, we have  $\Gamma_3 - 1 \simeq 2/3$  and the two terms compensate exactly. Therefore when the perturbation of the turbulent pressure is taken into account, the other terms should also be included and may not be neglected a priori. The variations of the non-diagonal components of the Reynolds stress tensor can

play also some role in the driving or damping, but we do not give here the expression for these terms (see Gabriel 1987). The weight of the different terms in Eq. (6) depends on the characteristics of the convection zone and the TDC theory adopted. We note for example that Balmforth (1992) and Houdek (2000) showed that the turbulent pressure variation plays the major role for the damping of the modes, using the TDC theory of Gough (1977). But we do not get the same conclusion with the TDC treatment of Gabriel (1996), as shown by Dupret et al. (2005a).

#### 4. PHOTOMETRIC AMPLITUDES AND PHASES AND MODE IDENTIFICATION

A crucial problem for the seismic study of auto-driven pulsators is the mode identification. First because, from a theoretical point of view, despite the linear non-adiabatic predictions, the mode selection mechanisms are not well understood for all the stars considered here. Second, because from an observational point of view, we do not resolve the disks of stars other than the Sun so that we can only observe disk-integrated quantities. Third, the rotational splittings and the “avoided crossing” effect produce such a complicated power spectrum that a mode identification based on the frequencies alone is generally impossible. It is thus essential to derive and improve mode identifications methods based on other observables, currently both spectroscopic and photometric techniques are being used. The latter methods are based on multi-colour photometry, and we consider them here with more details because they are closely related to energetic aspects of the oscillations.

The principle of these methods is to observe the photometric variations due to stellar oscillations in different colours and compare them to the theoretical predictions at the appropriate wavelengths (see e.g. Watson 1988, Garrido 2000). Some approximations are required to obtain a theoretical expression for the magnitude variations of pulsation modes:

- a1) The coupling of modes due to the interaction between rotation and pulsation is neglected. The angular dependence of a non-radial mode is thus described by a single spherical harmonic.
- a2) It is assumed that the visible part of the star, i.e. the photosphere, can be described by a single surface which is spherical at equilibrium. During the pulsation, it is assumed that the geometrical distortion of this surface follows the movement of the matter.
- a3) It is assumed that, during the pulsation cycle, the atmosphere adapts quasi-instantaneously its thermal and radiation structure to the changes due to the oscillations. Hence, the monochromatic outwards flux  $\vec{F}_\lambda$  and limb darkening law  $h_\lambda$  of the local atmosphere are assumed to be, for each given time, the

same as those of an equilibrium plane parallel atmosphere model with orientation deduced from the geometrical distortion (a2).

With these assumptions, an integration over the visible stellar disk can be performed analytically (Dziembowski 1977b, Stamford & Watson 1981), leading to the following expression for the monochromatic magnitude variations corresponding to a non-radial mode:

$$\delta m_\lambda = -\frac{2.5}{\ln 10} \epsilon P_\ell^m(\cos i) b_{\ell\lambda} \left( -(\ell-1)(\ell+2) \cos(\sigma t) + f_T \cos(\sigma t + \psi_T) (\alpha_{T\lambda} + \beta_{T\lambda}) - f_g \cos(\sigma t) (\alpha_{g\lambda} + \beta_{g\lambda}) \right), \quad (8)$$

In Eq. (8), the term proportional to  $(\ell-1)(\ell+2)$  corresponds to the influence of the stellar surface distortion, the term proportional to  $f_T$  corresponds to the influence of the local effective temperature variation and the term proportional to  $f_g$  corresponds to the influence of the local effective gravity variation.  $b_{\ell\lambda} = \int_0^1 h_\lambda \mu P_\ell d\mu$ , where  $h_\lambda$  is the limb-darkening law.  $\alpha_{T\lambda}$ ,  $\alpha_{g\lambda}$ ,  $\beta_{T\lambda}$  and  $\beta_{g\lambda}$  are logarithmic derivatives of the outward flux and  $b_{\ell\lambda}$  with respect to the effective temperature and gravity.

We stress two quantities in Eq. 8: the amplitude ( $f_T$ ) and phase ( $\psi_T$ ) of effective temperature variation for a normalized radial displacement. The important point is that they can only be determined by full non-adiabatic computations. The linear theory does not allow us to predict the amplitudes of the eigenfunctions. Therefore, it is appropriate to use amplitude ratios and phase differences between different filters when comparing theoretical predictions and observations. This comparison enables us to identify the degree  $\ell$  of the pulsation modes, but also to constrain  $f_T$  and  $\psi_T$ . Their knowledge enables us to probe energetic aspects of the oscillations and the physical description of the superficial non-adiabatic layers, as shown in the next section for different types of stars.

## 5. APPLICATIONS

### 5.1. $\beta$ Cephei stars

#### 5.1.1. Driving mechanism

$\beta$  Cephei stars are B0-B2.5 type multiperiodic pulsators with periods going from 3 to 8 hours. They are excellent targets for asteroseismology, as shown by Aerts (this conference).

The driving mechanism at the basis of the excitation of the  $\beta$  Cephei low order p and g-modes was explained

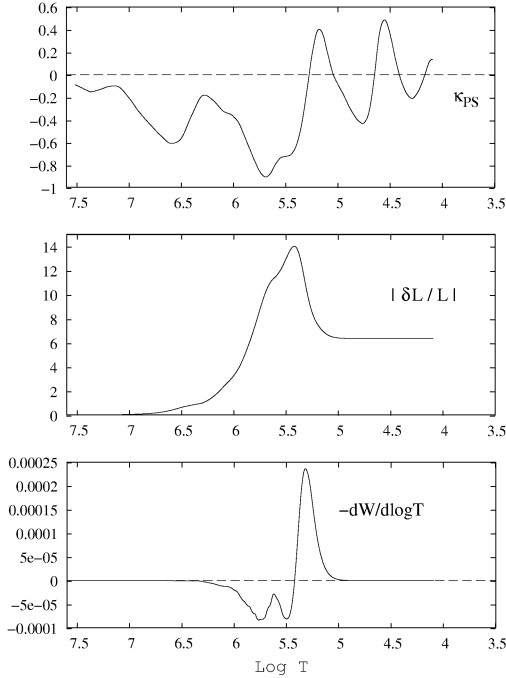


Figure 1. opacity derivative  $\kappa_{PS} = \partial \ln \kappa / \partial \ln P|_S$  (top), amplitude of luminosity variation  $|\delta L/L|$  (middle) and scaled work derivative  $-dW/d\log T$  (bottom), as a function of the logarithm of temperature, for the fundamental radial mode of a  $\beta$  Cep model with  $M = 9.5 M_{\odot}$ ,  $T_{\text{eff}} = 21750$  K and  $\log(L/L_{\odot}) = 3.877$ .

for example by Cox et al. (1992) when the new OPAL opacity tables (Iglesias & Rogers 1996) became available. These new computations lead to a significant increase of the opacity at temperatures around 200.000 K ( $\log T \simeq 5.3$ ) where a huge amount of iron transition lines are present. Non-adiabatic computations show that the significant opacity bump in this region leads to a classical  $\kappa$ -mechanism driving the oscillations. As the transition region for low order p-modes and g-modes is exactly located in this region for the hot  $\beta$  Cep stars, these modes are excited by this mechanism and no others.

We illustrate this driving mechanism in Fig. 1. In the transition region ( $\log T \simeq 5.3$ ),  $\kappa_{PS}$  is increasing outwards (top panel). As a consequence the luminosity variation decreases outwards (middle panel) and the energy is periodically blocked at the hot phase of pulsation. This energy is converted in positive mechanical work (bottom panel), which drives the oscillations. We note that the work curve in the bottom panel has been scaled in such a way that the area beneath the curve is the dimensionless growth rate. The region where it is positive (resp. negative) are driving (resp. damping) the oscillations.

Some important observational facts questioned recently our knowledge of the driving mechanism of  $\beta$  Cep modes. First, recent large multi-site campaigns, as for

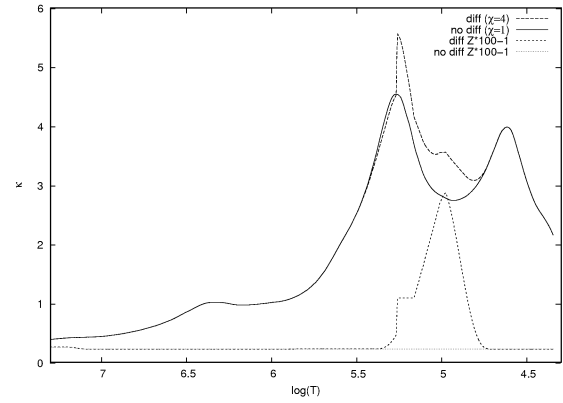


Figure 2. Comparison of opacities for a  $\beta$  Cep model with constant  $Z = 0.0122$  (solid line) and with diffusion and accumulation factor  $\chi = 4$  (dashed line). The values of  $100Z - 1$ , showing the accumulation of metals in the different layers are given at the bottom. Models with  $M = 10 M_{\odot}$ ,  $X = 0.7392$ ,  $T_{\text{eff}} = 23440$  K,  $\log(L/L_{\odot}) = 3.897$ .

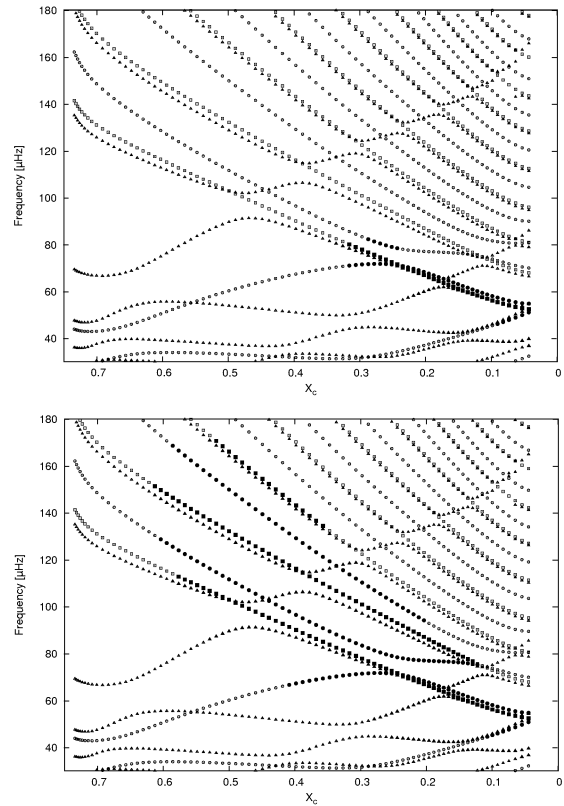


Figure 3. Evolution of frequencies [ $\mu\text{Hz}$ ] versus the central hydrogen mass fraction  $X_c$  for  $\beta$  Cep models with  $M = 10 M_{\odot}$  and  $X = 0.7392$ . Full (resp. empty) symbols correspond to unstable (resp. stable) modes. The top panel is for models with constant  $Z = 0.0122$ , the bottom panel is for models with diffusion and accumulation factor  $\chi = 4$  (same initial  $Z$ ). Figure from Bourge & Alecian (2006).

example for the star  $\nu$  Eridani (Handler et al. 2004), lead to the detection of many pulsation modes (see Aerts, these proceedings). Second,  $\beta$  Cep stars were recently discovered in the Large Magellanic Cloud (LMC) (Kolaczowski et al. 2004). The driving of some of these modes in the first case and of all the modes in the second is not explained by standard models with constant metallicity.

As the driving of the modes is associated with the iron opacity bump, we can search the answer in the metallicity. A first well known effect is that increasing the metallicity increases significantly the number of unstable modes and the size of the  $\beta$  Cephei instability strip (see Pamyatnykh 1999, Dupret 2002). However, global changes of the metallicity do not give the solution. Metallicities much larger than the spectroscopic values observed at the surface would be required. The problem is striking in the LMC where the surface metallicities are around  $Z = 0.008$ . Constant  $Z$  models with so small metallicities do not explain at all the driving of the  $\beta$  Cep modes.

Hence, additional effect(s) must be invoked to explain these observational facts. Following a basic idea of Cox et al. (1992), a promising effect that we consider here is the settling of heavy elements due to the conjuncted effect of microscopic diffusion, radiative forces and winds. Recent works by Bourge et al. (2006) and Bourge & Alecian (2006) show that a significant iron accumulation in the driving region can be expected due to these effects. This accumulation affects the iron opacity bump. This can be seen in Fig. 2, where we compare the opacities of  $\beta$  Cep models with constant  $Z$  and with metal enhancement in the driving region. The metal enhancement adopted here results of a parametric approach reflecting the profile expected from diffusion (linear extrapolation of elements flux), according to the definition of Bourge & Alecian (2006). Such differences of opacity modify strongly the driving of the modes. This is shown in Fig. 3, where we compare the stability of the modes obtained with and without metal enhancement. Many more modes are excited in the models with metal enhancement in the driving region. Such effects are sufficient to explain the driving of all modes of stars such as  $\nu$  Eri and the  $\beta$  Cep of the LMC.

### 5.1.2. Photometric amplitudes and phases

In the case of  $\beta$  Cep stars, the temperature-displacement phase-lag  $\psi_T$  is close to the adiabatic  $180^\circ$ . The comparison between the theoretical and observed multi-color photometric amplitude ratios is in general very successful: it allows the identification of the degree  $\ell$  of the pulsation modes and constraints can be obtained on  $f_T$  (see e.g. Dupret et al. 2003, 2004c; de Cat et al. 2006). In  $\beta$  Cep stars,  $f_T$  is very sensitive to the metallicity in the driving region. This can be understood as follows: increasing the metallicity makes the  $\kappa$ -mechanism more efficient, hence the luminosity variation drops more in

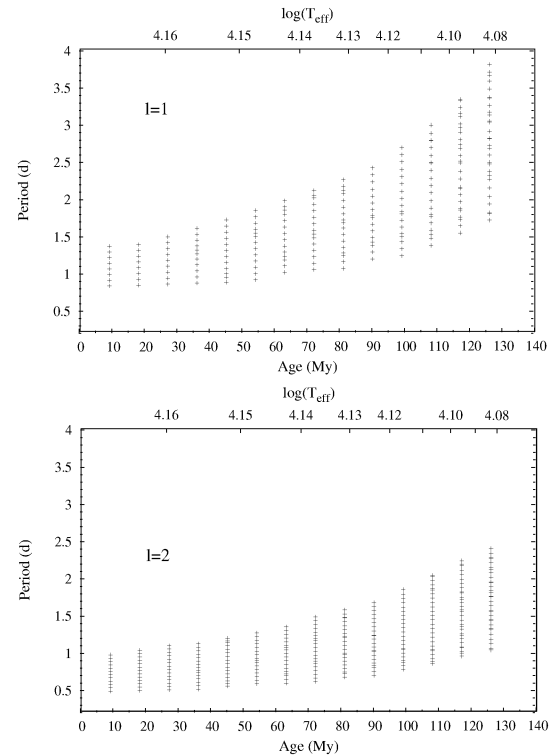


Figure 4. Periods of predicted SPB-type unstable g-modes of degree  $\ell = 1$  (top) and  $\ell = 2$  (bottom) along a  $4 M_\odot$ ,  $Z = 0.02$  evolutionary sequence (from ZAMS to TAMS).

the driving region (see Eqs. (3) and (4)). As  $\delta L/L = 4f_T + 2\delta r/r$  at the photosphere, this leads to smaller values of  $f_T$ . Hence, constraints on the metallicity can be obtained by comparing the theoretical and observed amplitude ratios, as shown by Dupret et al. (2003, 2004c) for the stars 16 Lac and HD 129929. We stress also the important work of Daszyńska et al. (2002) who showed that, in rapid rotators, the rotational coupling of the modes complicates a lot a correct interpretation of the observed amplitude ratios.

## 5.2. Slowly Pulsating B stars

### 5.2.1. Driving mechanism

The slowly pulsating B stars (SPB) are multiperiodic B3-B8 type main sequence stars with periods typically between 1 and 4 days corresponding to high order gravity modes (see Aerts, these proceedings). The driving mechanism at the basis of the excitation of the SPB g-modes is very similar to the one of the  $\beta$  Cep stars, as first explained by Dziembowski et al. (1993). Again, it is a  $\kappa$ -mechanism associated with the iron opacity bump around  $T = 200,000$  K. But this opacity bump is located deeper compared to the  $\beta$  Cep, because the SPB

are colder. Hence it coincides with the transition region for the high-order g-modes, and these modes are excited instead of the  $\beta$  Cep p-modes. As shown in Fig. 4, non-adiabatic theoretical models predict unstable modes with the appropriate range of period compared to observations. The period of unstable modes decreases with the degree  $\ell$ , as generally expected in g-modes for which the eigenfunctions are essentially function of  $\sigma^2/(\ell(\ell+1))$ . The number of predicted unstable modes is generally much larger than the number of observed frequencies in typical SPBs. But we emphasize the remarkable recent observations of the SPB star HD 163830 with the MOST (Microvariability and Oscillations of STars) satellite, which lead to the detection of about 20 frequencies (Aerts et al. 2006), indicating that many of the predicted unstable g-modes are present, but with smaller amplitudes. The observed instability strips is well reproduced by the theoretical models (Pamyatnykh 1999). For the same reasons as in the  $\beta$  Cep models, the driving of the SPB g-modes is very sensitive to the iron abundance. Iron accumulation due to the effect of radiative forces is expected to affect the period range of unstable modes. First works in this direction have been done by Miglio et al. (private communication), following a parametric approach for the iron enhancement.

Finally, works by Townsend (2005) including in non-adiabatic computations the effect of the Coriolis force (in framework of the “traditional approximation”) indicate that rotation shifts the theoretical SPB instability strip towards higher luminosities and effective temperatures and broadens its extent.

### 5.2.2. Photometric amplitudes and phases

In SPB stars,  $\psi_T$  is close to the adiabatic value  $0^\circ$  (g-modes). The comparison between the theoretical and observed multi-color photometric amplitude ratios allows often a successful identification of  $\ell$  (see e.g. Dupret et al. 2003; de Cat et al. 2005, 2006). In most of the cases, the modes detected in photometry are identified as  $\ell = 1$  modes. No  $\ell = 3$  modes have been photometrically detected and identified, in agreement with theoretical expectations (Townsend 2002). As in  $\beta$  Cep stars, the non-adiabatic theoretical predictions are sensitive to the metallicity, but to a smaller extent and the uncertainties are still too large to give strong constraints on it. The coupling of the spheroidal modes due to rotation is expected to be significant in these stars, because the rotation periods can be of the same order as the pulsation ones; and this could affect strongly the amplitude ratios. A method for the determination of the theoretical amplitude ratios, including this rotational coupling in the framework of the “traditional approximation” has been proposed by Townsend (2003). This study shows that, for all apart from prograde sectoral modes, the Coriolis force acts to trap the oscillation within an equatorial waveguide. As a consequence, unless viewed from near the poles, the variability of rapid rotators is predicted to be very small.

## 5.3. $\delta$ Scuti stars

### 5.3.1. Driving mechanism

$\delta$  Scuti stars are well known pulsating stars at the intersection region between the classical instability strip and the main sequence, their typical periods range from 0.5 to 6 hours. The driving mechanism of their low order p-modes is well known: it is a  $\kappa$ -mechanism occurring in the second partial ionization zone of Helium as for other stars of the classical instability strip (RR Lyrae, classical cepheids).

The location of the blue edge of the instability strip is well explained by this mechanism. For models inside the instability strip, the HeII partial ionization zone coincides with the transition region for low order p-modes and these modes are driven by the  $\kappa$ -mechanism. For hotter models, the HeII ionization zone is in more superficial layers and its driving effect on low order p-modes is smaller than the damping induced by deeper layers.

It is more difficult to explain the existence of a red edge to the instability strip. The key point is that towards the red side of the instability strip and for solar-calibrated values of the mixing-length parameter, the two thin convective zones associated with the HeII and H partial ionizations merge in a single larger convective envelope.

As mentioned in Sect. 2.1, an approximation frequently adopted in non-adiabatic modelling is to freeze the convection. However, this approximation is not acceptable towards the red side of the instability strip because in a significant part of the convective zone the time-scale associated with most energetic convective elements is smaller than the pulsation periods. As shown by Dupret et al. (2005a), in the frozen convection case, a flux blocking mechanism at the base of the convective envelope (comparable with the  $\gamma$  Dor case) takes the counterpart of the  $\kappa$ -mechanism and continues to drive the oscillations, so that no red edge is predicted with these models.

TDC treatments (see Sect. 2.1 and 3.2) are required and have been applied by different authors to explain the existence of the red edge of the  $\delta$  Scuti instability strip. Houdek (2000) studied the convective effects on radial p-mode stability in  $\delta$  Sct stars, using the TDC treatment of Gough (1977), together with the non-local treatment of Balmforth (1992). Xiong et al. (2001) obtained a theoretical red edge for radial modes, using the non-local TDC theory of Xiong et al. (1997). Dupret et al. (2004a, 2005a) succeeded obtaining a theoretical red edge for radial and non-radial modes, using the TDC treatment of Gabriel (1996) and Grigahcène et al. (2005).

We show in Fig. 5 the theoretical instability strips obtained for radial modes by Dupret et al. (2005a) and the red edges obtained by Xiong et al. (2001) and Houdek (2000) for the fundamental radial mode. The small points are the position of the  $\delta$  Sct stars of the Rodriguez et al. (2000) catalog, their effective temperatures were

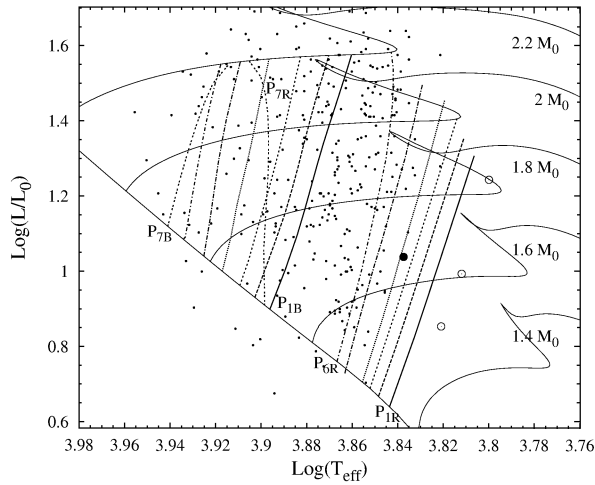


Figure 5. Blue and red edges of the  $\delta$  Sct theoretical IS. The lines are the TDC results obtained by Dupret et al. (2005a), for radial modes from  $p_1$  to  $p_7$ , for models with  $\alpha = 1.8$ . The small points correspond to observations. The empty and full bullet correspond to the red edges obtained by Xiong et al. (2001) ( $\odot$ ) and by Houdek (2000) ( $\bullet$ ) for the fundamental radial mode.

obtained using the calibrations of Moon & Dworetzky (1985).

In these different TDC treatments, it appears that the weight of the different terms appearing in Eq. (6) is different. For example, Houdek (2000) finds that the major contribution to the damping of the modes comes from the turbulent pressure variations, while Dupret et al. (2005a) find that the dissipation rate of turbulent kinetic energy variation counterbalances the effect of turbulent pressure variations and the main contribution to the damping comes from the convective flux variations. These differences indicate that still much work has to be done to understand the details of the damping mechanisms towards the red side of the instability strip.

### 5.3.2. Photometric amplitudes and phases

Mode identification is a crucial but difficult problem in  $\delta$  Sct stars. In these stars, both  $f_T$  and  $\psi_T$  are very sensitive to the non-adiabatic prescriptions and the detailed physical description of the superficial convective zone. Because of the uncertainties in the determination of these non-adiabatic quantities, they were considered for many years as free parameters for the comparison with observed multi-color photometric amplitude ratios and phase differences (Garrido 2000). But the reliability of the mode identification is much reinforced when full non-adiabatic computations are performed. Balona & Evers (1999) and Daszyńska et al. (2003) proceeded so, using the non-adiabatic code of Dziembowski (1977) in which the diffusion approximation is assumed. Dupret et al. (2003) and Moya et al. (2003) included the improved

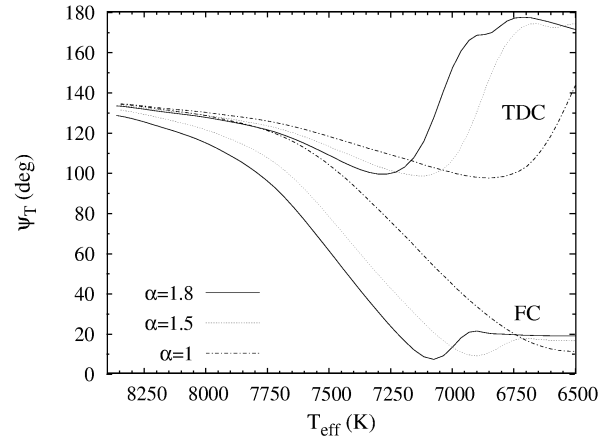


Figure 6. Evolution of the phase-lag  $\psi_T$  as a function of  $T_{\text{eff}}$ , for the fundamental radial mode, obtained with TDC and FC non-adiabatic models with  $M = 1.8 M_{\odot}$  and different  $\alpha$ .

perturbed atmosphere modeling of Dupret et al. (2002) in their computations. All these authors showed that, for  $\delta$  Sct stars the non-adiabatic theoretical predictions are very sensitive to the value adopted for the Mixing-Length (ML) parameter  $\alpha$ . The use of the convection theory of Canuto et al. (1996) has also been considered: Barban et al. (2003) computed new limb-darkening coefficients based on the atmosphere models by Heiter et al. (2002), and Dupret et al. (2004b) considered the inclusion of these new atmosphere models in their non-adiabatic computations. In all the above studies, a Frozen Convection (FC) approximation has been adopted.

Dupret et al. (2005c) applied for the first time a TDC treatment (Gabriel 1996; Grigahcène et al. 2005) to the determination of the photometric amplitude ratios and phase differences in  $\delta$  Sct stars. Fig. 6 compares the phase-lags predicted by FC and TDC non-adiabatic models, for different  $T_{\text{eff}}$ . We see that they are very different towards the red side of the instability strip; the explanation is given by Dupret et al. (2005c, Sect. 3). These authors show also that the amplitude ratios and phase differences predicted by TDC models much better agree with observations than the FC ones, particularly towards the red side of the instability strip. Hence, using TDC models allows a secure identification of the degree  $\ell$  of the modes, and opens the way to realistic seismic studies of  $\delta$  Sct stars

### 5.4. roAp stars

roAp stars are pulsating stars known for their chemical peculiarities, strong magnetic fields and rapid oscillations (periods between 4 and 16 min.). They present a very high interest for asteroseismology, giving a unique opportunity to probe the role of a strong magnetic field and its interaction with oscillation in stellar interiors, as shown



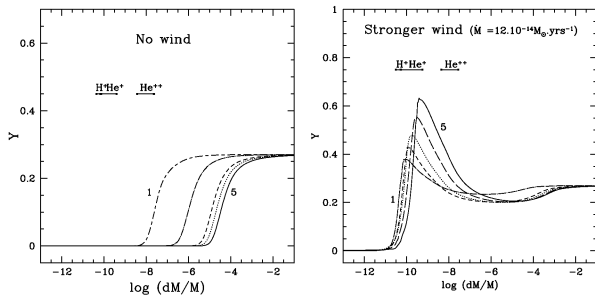


Figure 7. He profiles versus the outer mass fraction, for  $1.8 M_{\odot}$  models at different evolutionary stages from ZAMS to TAMS. Left panel is for models without winds and right panel for models with wind. Figure from Théado & Cunha (2006).

in the review of Kurtz (these proceedings).

The main driving of the roAp high order p-modes occurs in the H partial ionization zone, because it coincides with the transition region for these modes and the eigenfunctions amplitudes are too small in deeper layers. To explain the driving of the roAp modes, we first have to consider the effect of the magnetic field.

Works by Gough & Tayler (1966) and Balmforth et al. (2001) indicate that the strong magnetic field present near the magnetic poles of roAp stars possibly suppresses convective motions. Hence, a chemical stratification of elements is possible in the superficial regions due to the effects of microscopic diffusion and radiative forces. Théado & Cunha (2006) studied recently the combined effect of Helium settling and winds on the driving of the roAp modes. As shown in the left panel of Fig. 7, in models without winds, He simply sinks and the partial ionization zones of H and He become rapidly poor in helium and rich in hydrogen. As a consequence, the  $\kappa$ -driving of the roAp high-order modes is reinforced in the H ionization zone. But the  $\kappa$ -mechanism becomes inefficient in the HeII partial ionization zone and thus the  $\delta$  Sct-type low-order p-modes are stabilized (this effect was also studied by Balmforth et al. 2001). When a wind competes with He settling, helium accumulates in the HeI partial ionization zone. In this case, the roAp high-order modes are still excited, but the  $\kappa$ -driving in the HeII partial ionization zone is efficient enough to excite  $\delta$  Sct-type low-order p-modes.

Strong magnetic fields induce also a coupling of the spheroidal modes, throughout the action of the Lorentz force in the pulsation equations (see e.g. Saio & Gautschy 2004). A full non-adiabatic analysis was recently performed by Saio (2005), taking this coupling of the modes into account in a non-perturbative way (spherical harmonics expansion method with up to 12 components for each variable). He used models without diffusion and convective envelope. One result of this study is that the  $\delta$  Sct-type low-order p-modes and the radial high-order p-modes excited in the absence of magnetic field are stabilized if the polar strength of the dipole magnetic field is

larger than about 1 kG.

We emphasize that no  $\delta$  Sct-type low-order p-modes are detected in roAp stars, this indicates that the interaction with magnetic field plays an effective role in the driving and damping of the modes and that no strong winds leading to He accumulation are present in roAp stars.

## 5.5. $\gamma$ Doradus stars

### 5.5.1. Driving mechanism

Just at the right and partially inside the instability strip of  $\delta$  Scuti stars, a new class of variable pulsating stars was discovered about 10 years ago: the  $\gamma$  Doradus stars. These stars have long periods (between 0.35 and 3 days) corresponding to high-order gravity modes.

The driving mechanism of the  $\gamma$  Dor gravity modes has been a matter of debate during the last decade. A key point is that the transition region where the pulsation periods of high order g-modes are of the same order as the thermal relaxation time is near the bottom of the Convective Envelope (CE) in  $\gamma$  Dor stars. This lead Guzik et al. (2000) to explain as follows the driving of the  $\gamma$  Dor g-modes. The radiative luminosity drops suddenly at the bottom of the convective zone. Therefore, at the hot phase of pulsation, the increasing energy flux coming from below the convection zone cannot be transported by radiation inside it. If we admit that the convective flux does not adapt immediately to the changes due to oscillations, the energy is thus periodically blocked in this region and transformed in mechanical work leading to the oscillations (see Eq. (3)).

Guzik et al. (2000) used the Frozen Convection approximation in their non-adiabatic models. In a very thin region near the bottom of the convection zone, the life-time of the convective elements is larger than the pulsation periods and the FC approximation is acceptable there; but it is the contrary in the rest of the convection zone. Hence, it is crucial to determine the exact role played by Time-Dependent Convection (TDC) in the driving mechanism of  $\gamma$  Dor stars. This role was studied by Dupret et al. (2004a, 2005a), using the TDC treatment of Gabriel (1996) and Grigahcène et al. (2005). This treatment takes the time-variations of the convective flux ( $\delta \vec{F}_c$ ), the turbulent pressure ( $\delta p_t$ ) and the dissipation rate of turbulent kinetic energy ( $\delta \epsilon_2$ ) into account.

In Fig. 8, we give the total work integral (curve 7) obtained with our TDC treatment for a typical  $\gamma$  Dor g-mode and a structure model with  $M = 1.6 M_{\odot}$ ,  $T_{\text{eff}} = 6935$  K,  $\log(L/L_{\odot}) = 0.96$  and  $\alpha = 2$ . Regions where the work integral increases (resp. decreases) have a driving (resp. damping) effect on the oscillations. It is normalized in such a way that the surface value is the dimensionless growth-rate:  $\eta \sqrt{R^3/GM}$ . We also give in this figure the contributions of different TDC terms, according to

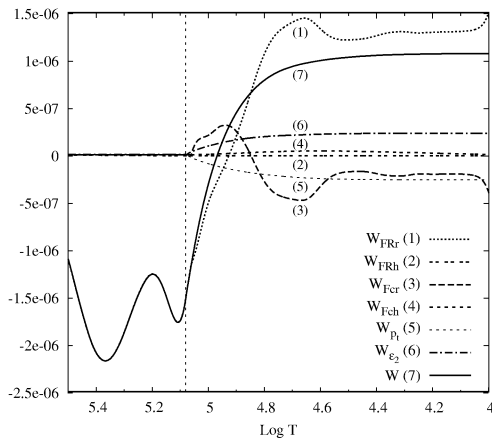


Figure 8. Different physical components of the work integral obtained with our TDC treatment for the mode  $\ell = 1$ ,  $g_{50}$ , for a typical  $\gamma$  Dor model with  $\alpha = 2$ . The vertical line is the CE base.

Eq. (6). In particular we give the contributions of the radial and transversal components of the radiative and convective flux perturbations. We see that significant driving occurs at the CE base for the mode  $\ell = 1$ ,  $g_{50}$  (Curve 7). Decomposition in radiative and convective flux contributions shows that the convective flux variations do not play a significant role at the CE base (Curve 3). The main driving comes from the radiative flux variations (Curve 1) which supports the flux blocking mechanism proposed by Guzik et al. (2000). We see also in Fig. 8 that the transversal components of radiative and convective flux variations (Curves 2 and 4) do not play a significant role in the work integral, due to the fact that the horizontal wavelength ( $r/(\ell(\ell + 1))$ ) is much larger than the scale heights of the different physical quantities in the superficial layers of the star. The contribution of  $\delta p_t$  and  $\delta \epsilon_2$  on the work integral are given in Curves 5 and 6 respectively. We see that these terms have an opposite effect, so that the work integral that includes all the perturbed convection terms is close to the one with only the perturbed convective flux.

In Fig. 9, we show the periods range of the unstable modes predicted by our TDC models as a function of the effective temperatures for main sequence models of  $1.6 M_{\odot}$  with Mixing-Length (ML) parameter  $\alpha = 2$  and  $\ell = 1$  modes. The periods range and the effective temperatures for the unstable g-modes are in agreement with the typical observed periods in  $\gamma$  Dor stars for this value of  $\alpha$ . As for the SPB stars, the predicted number of unstable g-modes is much larger than what is typically observed in  $\gamma$  Dor stars. But we expect the number of detected modes to be significantly increased in the forthcoming years, thanks to observations from space with e.g. COROT.

Theoretical instability strips for the  $\gamma$  Dor g-modes have been computed by Warner et al. (2003) using FC treatment and by Dupret et al. (2004a, 2005a) using the

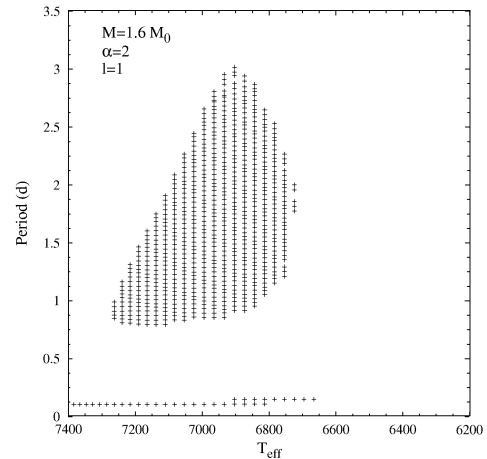


Figure 9. Periods (in days) of the unstable gravity modes as a function of  $T_{\text{eff}}$  obtained for TDC models of  $1.6 M_{\odot}$  with  $\alpha = 2$ . Each cross corresponds to a given  $\ell = 1$  mode.

Gabriel's treatment. A good agreement with the observed instability strip can be obtained for MLT parameter  $\alpha \simeq 2$  (near the solar calibrated value). As shown by Dupret et al. (2004a, 2005a), the theoretical instability strip is displaced towards lower effective temperatures when  $\alpha$  is decreased, simply because the size of the convective envelope (key point for the driving) is directly related to  $\alpha$ .

The stability of high-order g-modes at the red side of the  $\gamma$  Dor instability strip and of the modes of intermediate radial order (modes with periods between 0.15 and 0.8 days in Fig. 9) is explained by a radiative damping mechanism occurring in the g-mode cavity. More precisely, in these two cases, the eigenfunctions have spatial oscillations with large amplitudes in the g-mode cavity. Hence, the radiative damping in this region is much larger than the excitation near the base of the convective envelope. We refer to Dupret et al. (2005a) for more details about this damping mechanism.

As a summary, the g-mode cavity always has a stabilizing (damping) influence, while the flux blocking at the bottom of the CE has a destabilizing (driving) one. The balance between these two mechanisms explains the exact location of the  $\gamma$  Dor instability strip.

Finally, we emphasize that our TDC models predict the existence of stars having simultaneously unstable high-order gravity modes of  $\gamma$  Dor type and unstable low-order p-g modes of  $\delta$  Sct type. The detection of stars with such hybrid behaviour would present a very high interest for asteroseismology: their high-order g-modes would enable us to probe the very deep layers of the star and their low-order p-g modes would enable us to probe the intermediate and superficial layers. Much observational effort has been performed to detect such hybrid stars and two have been discovered: HD 209295 (Handler et al. 2002) and HD 8801 (Henry & Fekel 2005). We refer to Grihacène et al. (2006) for more details about this aspect.

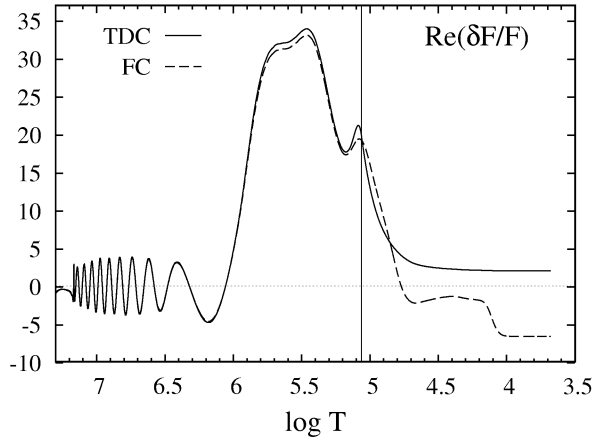


Figure 10.  $\Re\{\delta F/F\}$  (relative variation of the radial component of the total flux) as a function of  $\log T$ , obtained with TDC and FC treatments, for the mode  $\ell = 1$ ,  $g_{22}$  ( $f = 1.192$  c/d), model with  $M = 1.55 M_{\odot}$ ,  $T_{\text{eff}} = 7020$  K,  $\log(L/L_{\odot}) = 0.872$ . The vertical line gives the bottom of the convective envelope.

### 5.5.2. Photometric amplitudes and phases

The mode identification is an important but difficult problem in  $\gamma$  Dor stars. In these stars, both  $f_T$  and  $\psi_T$  are very sensitive to the non-adiabatic prescriptions and the detailed physical description of the superficial convective zone. Observations of the multi-color photometric amplitude ratios indicate that  $f_T$  is very small in  $\gamma$  Dor stars, which is somehow surprising for g-modes (Aerts et al. 2004; Dupret et al. 2005b). Simultaneous spectrophotometric observations were performed for well known stars such as  $\gamma$  Doradus itself (Balona et al. 1996). From these observations, light-displacement phase-lags between  $-25^{\circ}$  and  $-80^{\circ}$  were deduced.

Dupret et al. (2005b) applied FC and TDC treatments to the mode identification of five  $\gamma$  Dor stars. They showed that a much better agreement can be obtained between the observed multi-color photometric amplitude ratios and the theoretical TDC predictions, compared to FC predictions. They also showed that the phase-lags  $\psi_T$  predicted by TDC models are typically between  $-20^{\circ}$  and  $-40^{\circ}$  for  $\ell = 1$  modes, in reasonable agreement with observations. But the FC theoretical phase-lags around  $180^{\circ}$  are in complete disagreement with observations. This shows that TDC models must be used for realistic photometric mode identification in  $\gamma$  Dor stars.

In order to explain the very different phase-lags predicted by TDC and FC non-adiabatic models, we give in Fig. 10 the real part of  $\delta F/F$  as a function of  $\log T$ , obtained with TDC (solid line) and FC (dashed line) treatments. This eigenfunction is normalized so that the relative radial displacement is 1 at the photosphere. In both cases,  $\Re(\delta F/F)$  drops near the base of the Convective Envelope ( $\log T \simeq 5$ ). This corresponds to the flux blocking mech-

anism described in details in previous section. In the FC case,  $\kappa$ -mechanism occurs inside the convective envelope (CE), in the partial ionization zones of HeII ( $\log T \simeq 4.8$ ) and H ( $\log T \simeq 4.1$ ). These  $\kappa$ -mechanisms imply additional drops of  $\Re(\delta F/F)$  down to negative values, which explains the phase-lags around  $180^{\circ}$  predicted by the FC models. In contrast, these  $\kappa$ -mechanisms inside the CE are not allowed by TDC models, because they would lead to too high superadiabatic gradients. Therefore,  $\delta F/F$  remains flat and positive after the flux blocking drop and its phase remains around  $0^{\circ}$ .

## 6. CONCLUSIONS

We have considered in this paper energetic aspects of the oscillations in different main sequence auto-driven pulsators. In  $\beta$  Cep and SPB stars, the  $\kappa$ -driving is associated with the iron opacity bump. Iron accumulation due mainly to the effect of radiative forces can reinforce significantly this driving. Comparison between theoretical and observed multi-color photometric amplitude ratios allows the mode identification and constrains the metallicity. For  $\delta$  Sct stars, time-dependent convection (TDC) models are required to reproduce the red edge of the instability strip and to allow secure photometric mode identification in this region. In roAp stars, the  $\kappa$ -driving occurs in the H ionization zone. Convection is expected to be partially suppressed by the magnetic field, allowing diffusion to take place and reinforce the driving. The driving of the  $\gamma$  Doradus g-modes is due to a periodic flux blocking at the base of the convective envelope. TDC models are required for their photometric mode identification.

## ACKNOWLEDGMENTS

MAD acknowledges financial support by the CNRS. ST was supported by ESA-PRODEX grant C90135. POB acknowledges support through the Belgian Interuniversity Attraction Pole grant P5/36.

## REFERENCES

- [1] Aerts, C., Cuypers, J., De Cat, P., Dupret, M.-A., et al., 2004, *A&A*, 415, 1079
- [2] Aerts, C., de Cat, P., Kuschnig, R., Matthews, J. M., et al., 2006, *ApJ*, 642, L165
- [3] Balmforth, N.J., 1992, *MNRAS*, 255, 603
- [4] Balmforth, N.J., Cunha, M. S., Dolez, N., et al., 2001, *MNRAS*, 323, 362
- [5] Balona L. A., Böhm T., Foing B. H., Ghosh K. K., Janot-Pacheco E., Krisciunas K., Lagrange A.-M., Lawson W. A. et al., 1996, *MNRAS*, 281, 1315
- [6] Balona, L.A., Evers, E.A., 1999, *MNRAS*, 302, 349

- [7] Barban C., Goupil M. J., Van't Veer-Menneret C. et al., 2003, *A&A*, 405, 1095
- [8] Bourge, P. O., & Alecian, G., 2006, In: *Astrophysics of Variable Stars*, eds. C. Sterken and C. Aerts, ASP Conference Series, 349, 201
- [9] Bourge, P. O., Alecian, G., Thoul, A., et al., 2006, *CoAst*, 147, 105
- [10] Canuto V. M., Goldman I., Mazzitelli I., 1996, *ApJ*, 473, 550
- [11] Cox, A.N., Morgan, S.M., Rogers, F.J., Iglesias, C.A., 1992, *ApJ*, 393, 272
- [12] Daszyńska-Daszkiewicz, J., Dziembowski, W.A., Pamyatnykh, A.A., Goupil, M.-J., 2002, *A&A* 392, 151
- [13] Daszyńska-Daszkiewicz J., Dziembowski W. A., Pamyatnykh A. A., 2003, *A&A*, 407, 999
- [14] de Cat, P., Briquet, M., Daszyńska-Daszkiewicz, J., Dupret, M.-A., et al., 2005, *A&A* 432, 1013
- [15] de Cat, P., Briquet, M., Aerts, C., et al., 2006, submitted to *A&A*
- [16] Dupret, M.-A., De Ridder, J., Neuforge, C., Aerts, C., and Scuflaire R., 2002, *A&A* 385, 563
- [17] Dupret M.-A., De Ridder J., De Cat P. et al., 2003, *A&A*, 398, 677
- [18] Dupret, M.-A., Grigahcène, A., Garrido, R., et al., 2004a, *A&A*, 414, L17
- [19] Dupret M.-A., Montalban J., Grigahcène A. et al., 2004b, In: *Variable Stars in the Local Group*, eds. D.W. Kurtz & K. Pollard, PASP Conference Series, 310, 470
- [20] Dupret M.-A., Thoul, A., Scuflaire, R., et al., 2004c, *A&A*, 415, 251
- [21] Dupret, M.-A., Grigahcène, A., Garrido, R., et al. 2005a, *A&A*, 435, 927
- [22] Dupret, M.-A., Grigahcène, A., Garrido, R., et al. 2005b, *MNRAS*, 360, 1143
- [23] Dupret, M.-A., Grigahcène, A., Garrido, R., et al., 2005c, *MNRAS*, 361, 476
- [24] Dupret, M.-A., Goupil, M.-J., Samadi, R. et al., these proceedings, paper II
- [25] Dziembowski, W., 1977a, *Acta Astron.* 27, 95
- [26] Dziembowski, W., 1977b, *Acta Astron.* 27, 203
- [27] Dziembowski, W.A., Moskalik, P., Pamyatnykh, A.A., 1993, *MNRAS*, 265, 588
- [28] Gabriel, M., 1987, *A&A*, 175, 125
- [29] Gabriel, M. 1996, *Bull. Astron. Soc. of India* 24, 233
- [30] Garrido, R., 2000, In: *The 6th Vienna Workshop on  $\delta$  Scuti and related stars*, eds. M. Montgomery, M. Breger, PASP Conference Series, 210, 67
- [31] Gough, D. O., & Tayler, R. J., 1966, *MNRAS*, 133, 85
- [32] Gough, D. O., 1977, *ApJ*, 214, 196
- [33] Grigahcène, A., Dupret, M.-A., Gabriel, M., et al. 2005, *A&A* 434, 1055
- [34] Grigahcène, A., Martin-Ruiz, S., Dupret, M.-A., et al., 2006, *Mem. Soc. Astron. Ital.*, 77, 559
- [35] Guzik, J. A., Kaye, A. B., Bradley, P. A., et al. 2000, *ApJ*, 542, L57
- [36] Kolaczowski, Z., Pigulski, A., Soszynski, I., et al., 2004, In: *Variable Stars in the Local Group*, eds. D.W. Kurtz & K. Pollard, PASP Conference Series, 310, 225
- [37] Handler, G., Balona, L. A., Shobbrook, R. R., et al., 2002, *MNRAS*, 333, 262
- [38] Handler, G., Shobbrook, R. R., Jerzykiewicz, M., et al., 2004, *MNRAS*, 347, 454
- [39] Heiter U., Kupka F., van't Veer-Menneret C. et al., 2002, *A&A*, 392, 619
- [40] Henry, G. W., & Fekel, F. C. 2005, *AJ*, 129, 2026
- [41] Houdek, G. 2000, In: *The 6th Vienna Workshop on  $\delta$  Scuti and related stars*, eds. M. Montgomery, M. Breger, PASP Conference Series, 210, 454
- [42] Iglesias, C.A., & Rogers, F.J., 1996, *ApJ*, 464, 943
- [43] Kurucz, R.L., 1993, *ATLAS9 Stellar Atmosphere programs and 2 km/s grids*. Kurucz CDROM No 13
- [44] Moon, T. T., & Dworetzky, M. M. 1985, *MNRAS*, 217, 305
- [45] Moya, A., Garrido, R., Dupret, M.-A., 2004, *A&A*, 414, 1081
- [46] Pamyatnykh, A.A., 1999, *Acta Astron.* 49, 119
- [47] Rodriguez, E., Lopez-Gonzalez, M. J., & Lopez de Coca, P. 2000, *A&AS*, 144, 469
- [48] Saio, H., & Cox, J.P., 1980, *ApJ*, 236, 549
- [49] Saio, H., & Gautschy, A., 2004, *MNRAS*, 350, 485
- [50] Saio, H., 2005, *MNRAS*, 360, 1022
- [51] Samadi, R., Nordlund, A., Stein, R. F., et al., 2003, *A&A*, 404, 1129
- [52] Stamford, P.A., Watson, R.D., 1981, *Ap&SS* 77, 131
- [53] Stein, R. F., & Nordlund, A. 1998, *ApJ*, 499, 914
- [54] Théado, S., & Cunha, M. S., 2006, *CoAst*, 147, 101
- [55] Townsend, R., 2002, *MNRAS* 330, 855
- [56] Townsend, R., 2003, *MNRAS*, 343, 125
- [57] Townsend, R., 2005, *MNRAS*, 360, 465
- [58] Warner, P. B., Kaye, A. B., & Guzik, J. A. 2003, *ApJ*, 593, 1049
- [59] Watson, R.D., 1988, *Ap&SS* 140, 255
- [60] Xiong, D. R., Cheng, Q. L., & Deng, L. 1997, *ApJS*, 108, 529
- [61] Xiong, D. R., & Deng, L. 2001, *MNRAS*, 324, 243